# Removal of U(VI) in the Alkaline Conditions Created by $NH_3$ Gas-17288

Claudia Cardona[a], Yelena Katsenovich[a], Jim Szecsody[b], Leonel Lagos

[a]Applied Research Center, Florida International University, 10555 W. Flagler Street, Miami, FL 33174, USA

[b]Pacific Northwest National Laboratory, PO Box 999, K3-62, Richland, WA 99352

## ABSTRACT

Injection of ammonia ($NH_3$) gas in the unsaturated zone is an innovative technology to mitigate uranium contamination in the presence of oxygenated, high-carbonate, alkaline soil, and pore water composition typical for the Hanford Site. A uranium-contaminated plume is a potential source for groundwater pollution due to migration of soluble uranium species towards the water table. This study evaluates the effect of various pore water constituents such as Ca, Al, Si and bicarbonate ions on changes in uranium concentrations in alkaline conditions, created by the injection of $NH_3$ gas to be used to effectively mitigate uranium contamination in the vadose zone sediments. The main target in this research was the speciation modeling calculations conducted via the Geochemist Workbench (GWB) software. For this purpose, the GWB's database was updated with the most recently published U thermodynamic data on dissolution reactions and revised stability and solubility product constants. The simulations were carried out for varied pore water compositions with 5% of $NH_3$(g) to increase the initial pore water pH from 8.0 to 11.87. The model assumed the system is closed to the atmosphere; so, no exchange of $CO_2$ with the atmosphere. The predicted U(VI) aqueous species and saturation indices [SI= log(IAP/$K_{sp}$)] were plotted as a function of pH values. The aqueous uranium carbonate species, $UO_2(CO_3)_2^{4-}$ and $UO_2(CO_3)_2^{2-}$, were more abundant in the absence of $Ca^{2+}$ and at a low bicarbonate concentration. In pore water compositions containing $Ca^{2+}$ and $HCO_3^-$, the major predicted aqueous species were $Ca_2UO_2(CO_3)_3^0$, $CaUO_2(CO_3)_2$, and $UO_2(CO_3)_3^{-4}$. Also, the speciation modeling predicted the formation of boltwoodite [Na,K($H_3O$) $UO_2(SiO_4)$], uranophane [$Ca(UO_2)_2(HSiO_4)_2$ $5H_2O$], and grimselite [$NaK_3UO_2(CO_3)_3$·H2O] minerals. The computed saturation indices (SI) indicated saturation of boltwoodite minerals in the simulated Ca-free compositions at zero and low (0 and 2.9 mM) $HCO_3^-$ concentrations. In the presence of Ca ions, 5mM and 10mM, and similar $HCO_3^-$ concentrations, speciation modeling predicted the formation of uranophane. However, grimselite phase was prevailing when simulated solutions contained $Ca^{2+}$ ions and higher bicarbonate concentrations of 50mM.

## INTRODUCTION

At the Hanford Site, a significant residual mass of the disposed uranium inventory still resides in the deep vadose [1]. The mobility of uranium in the oxidizing, carbonate-rich Hanford subsurface at pH ~8.0 is relatively high, with a low U(VI) adsorption distribution coefficient ($K_d$) averaging 0.11 - 4 L/kg [1],[2],[3]. The mobility of U(VI) is explained by the formation of highly soluble and stable uranyl-carbonato complexes ($UO_2CO_3^0$, $UO_2(CO_3)_2^{2-}$ and $UO_2(CO_3)_3^{4-}$) [4], [5] Remediation techniques for the deep VZ contaminated with radionuclides have so

far received less attention although such methods are critical for protection of water resources from contaminants historically accumulated in the unsaturated subsurface environments. Remediation of deep vadose zone contamination of radionuclides can potentially be done in-situ by converting aqueous U-carbonate mobile phases to lower solubility precipitates that are stable in the natural environment.

Injection of $NH_3$ gas to the vadose zone is a viable method to decrease uranium mobility in the contaminated subsurface via pH manipulation and creation of alkaline conditions [6]. Ammonia is a highly soluble gas and its injection in the vadose zone can cause the formation of $NH_4^+$ (which consumes $H^+$) in pore water followed by a subsequent increase in pH up to 11.87 (3.1 mol/L $NH_3$ (aq)) for 5% $NH_3$. This manipulation can significantly alter the pore water chemistry due to dissolution of the dominant soil minerals such as calcite, feldspar, iron oxides, and quartz present in the VZ soil. These dissolution reactions in alkaline conditions potentially induce the release of cations including Si, Al, Ca, Mg, Na, and K from soil minerals to pore water [7]. Then, upon the re-establishment of natural pH conditions, various silica and aluminosilicate solid phases would precipitate as a uranium-silicate such as Na-boltwoodite or coat U-bearing phases forming a low solubility, non-U precipitate, such as cancrinite [8]), sodalite, hydrobiotite, brucite, and goethite, as observed in water-saturated systems [9], [10]. These chemical reactions can potentially control the mobility of uranyl cations and limit their downward migration to the underlying groundwater aquifer. However, there is a lack of knowledge on how pore water constituencies in alkaline conditions where soil minerals dissolution contributes to the solution ions may affect uranium removal or precipitation.

The focus of this study was to perform speciation modeling simulations to correlate results with SEM/EDS and XRD analysis on the selected precipitate samples. The speciation modeling for the prediction of uranium aqueous species and solid phases has included a literature search to manually edit thermodynamic datasets in the Geochemist Workbench (GWB) software. This research was extended to obtain SEM/EDS images for uranium elevated samples followed by XRD analysis to find a correlation with the speciation modeling predictions.

## MATERIAL AND METHODS

### Sample Preparation

The composition of pore water at the Hanford Site has been previously characterized in terms of concentrations of major cations, anions, and pH [11] For the purpose of this research, the pore water composition was simplified to have five major components in the test solutions: uranium, silica, aluminum, calcium and bicarbonate. The concentration of uranium in all experiments was kept constant at 0.0084 mM (2 mg/L) [12] and the bicarbonate concentrations varied from 0 to 100 mM (0, 2.9, 25, 50, 75 and 100 mM). The silica concentration was tested in the range of 5mM to 250mM (5, 50, 100, 150, 200, 250 mM) given past observations of 30 mM silica in 5% $NH_3$ treated sediment [6] and up to 100mM silica in 10% $NH_3$ treated sediment [13] The same maximum Si concentration (100mM) with the total cation value of 250 mM was noted by Szecsody [14]. Past observations also showed that the concentration of Al released during the soil treatment by 1 mol $L^{-1}$ NaOH is

relatively small, resulting in ~5.1 mM of Al in the soil solution [15], justifying the fact that Al concentrations are smaller than Si. Both Si and Al concentrations tested for these experiments are orders of magnitude greater than U; that can lead to the potential U precipitation as U-silicates from the Si and Al amended synthetic solutions.

The calcite mineral is abundant in Hanford soil and it exists as a mineralogical component in all subsurface sediments [16]. Groundwater and pore water are in equilibrium with calcite, which exists in the form of caliche layers. The concentration of calcium carbonate in these layers varies over a wide range [17], justifying the wide range of bicarbonate concentrations tested in the experiments. Stock solutions of Al (50 mM), Si (422 mM), and $HCO_3^-$ (400 mM) were first prepared in deionized water (DIW) from the salts $Al(NO_3)_3 \cdot 9H_2O$, $Na_2SiO_3 \cdot 9H_20$, and $KHCO_3$, respectively, reaching the desired concentrations in 50 mL volume. Sodium metasilicate ($Na_2SiO_3 \cdot 9H_20$) and potassium bicarbonate ($KHCO_3$) served as a source of sodium and potassium in the solution mixture. Experimental results on the removal of uranium were presented in previous reports and publications [12].

In addition, a set of samples was prepared with elevated uranium concentrations for SEM/EDS analysis. The same procedures for sample preparation as previously described for samples containing 2 ppm of U were followed, except for the uranium concentration that was injected (400 ppm). These solutions were consistent across the samples with the only differences being the bicarbonate ($HCO_3^-$) and calcium ($Ca^{2+}$) content added. The concentrated stock solutions were prepared such that the final desired sample concentration would be reached after mixing in the stock solutions.

## Geochemical Modeling for Speciation Prediction

The Geochemist Workbench (GWB) version 10.0 [17]. React Module was used to predict aqueous speciation and mineral phases likely to be saturated in the post-treated synthetic pore water after ammonia gas injections. The React Module allowed for varying the pH levels, simulating the addition of ammonia. The GWB software compiles four thermodynamic databases for speciation models. The Visual MINTEQ version 2.40 thermodynamic database, thermo-minteq.tdat, formatted for the GWB by Jon Petter Gustafsson (KTH Royal Institute of Technology), was chosen to run simulations. This database was manually updated to include some uranyl aqueous species and solid phases along with revision of their stability constants and solubility products (log K's) at 25 ºC. Critically reviewed thermodynamic databases with a reliable data selection on uranium aqueous and solid phases were taken from the National Cooperative for the Disposal of Radioactive Waste [18] and the Thermodynamic Reference Database (THEREDA) for Nuclear Waste Disposal [19]), which reviewed the most recently published peer-reviewed publications [5], [20], [21], [22],[23], [24], [25], [26], [27].

Simulations were carried out for the six initial pore water compositions using the GWB speciation modeling software. The simulated synthetic pore water (SPW) compositions contained 2 ppm (0.0084mM) of $UO_2^{2+}$; Si and Al concentrations were kept constants at 50mM and 5mM respectively; low (2.9mM) and high (50mM) $HCO_3^-$ concentrations; and 0, 5, and 10mM of $Ca^{2+}$.

This modeling was conducted for a system closed to the exchange of $CO_2$ with the atmosphere. A closed system is also more applicable to field treatment where the 95% $N_2$, 5% $NH_3$ gas will be injected into a zone. With a $NH_3$ gas retardation of 300 to 400 depending on water content [6] there will eventually be a large zone where the pore gas is flushed out and replaced with $N_2$ as well as a smaller zone where $NH_3$ gas is in equilibrium with ammonia in the pore water. This effectively is a closed system in terms of $CO_2$ partitioning, at least for the short term (i.e., several months). Over a longer time-span (i.e., years), due to gas diffusion, atmospheric gas will eventually equilibrate with the treated zone. The simulated pore water solutions included five cations and three anions at an initial pH of 8. The $H_2SiO_4^{2-}$ was assumed to represent all the silica species in the solution at 25ºC [20]. Dissolved oxygen was set as 8.4 mg/L at a constant temperature 25ºC and the concentration of U(VI) was kept constant at 2 mg/L in all simulations. In the Reactants pane, experimental conditions were simulated by sliding pH from 8 to 11.87 for 5% of $NH_3$(g). This would result in the React Module simulating the concentration of aqueous ammonia as 3.1mol/L in the solutions at equilibrium. The aqueous uranium species and minerals uranium species were identified and graphed as a function of the pH. These speciation models assumed that ammonia would not reduce U(VI) to U(IV).

### SEM-EDS Analysis

Scanning electron microscopy and energy dispersive spectroscopy (SEM-EDS) were used to study the surface morphology and composition of precipitates formed during sample preparation. The recovered solids were allowed to dry in preparation for SEM-EDS and X-ray diffraction analysis. Small specimens were taken from the solid precipitates and mounted to aluminum studs covered with double-sided carbon tape. The SEM system used was a JOEL-5910-LV with acceleration potentials ranging from 10 to 20 kV. EDS analysis was produced using an EDAX Sapphire detector with UTW Window controlled through Genesis software. Any required gold coating was done with an SPI-Module Control and Sputter unit for 2 minutes to produce a thin layer of gold. The specimens were coated with gold and palladium to enhance conductivity and were analyzed in backscatter electron capture mode, which is preferred for distinguishing the differences in average atomic weight in an area. This was of particular use to this study for identifying areas of elevated uranium content. The uranium content was also associated with other elements in the sample composition, such as silica, sodium or calcium.

## RESULTS AND DISCUSSION

### Geochemical Modeling Results, Ca-free synthetic solutions

GWB speciation modeling helped to predict uranium aqueous species and uranium-mineral phases that might form in varied pore-water compositions after ammonia gas injection in the subsurface. The predominant aqueous species and the mineral saturation indices (Q/K) with $UO_2^{2+}$ were displayed as a function of pH. According to the speciation modeling, in bicarbonate–free synthetic solutions, $UO_2(OH)_3^-$ and $UO_2(OH)_4^{2-}$ were the predominant aqueous uranium species. In the presence of bicarbonate, aqueous uranium carbonates species, $UO_2(CO_3)_3^{4-}$ and $UO_2(CO_3)_2^{2-}$, dominated uranium speciation and the concentration of uranyl carbonates species was noted to decrease above pH 9.5 (Figure 1-B1). At higher bicarbonate

concentrations, the concentration of $UO_2(CO_3)_3^{4-}$ species was almost unchanged over a pH range from 8 to 11; but then at pH above 11.5, their concentrations were slightly decreased (Figure 1- C1).

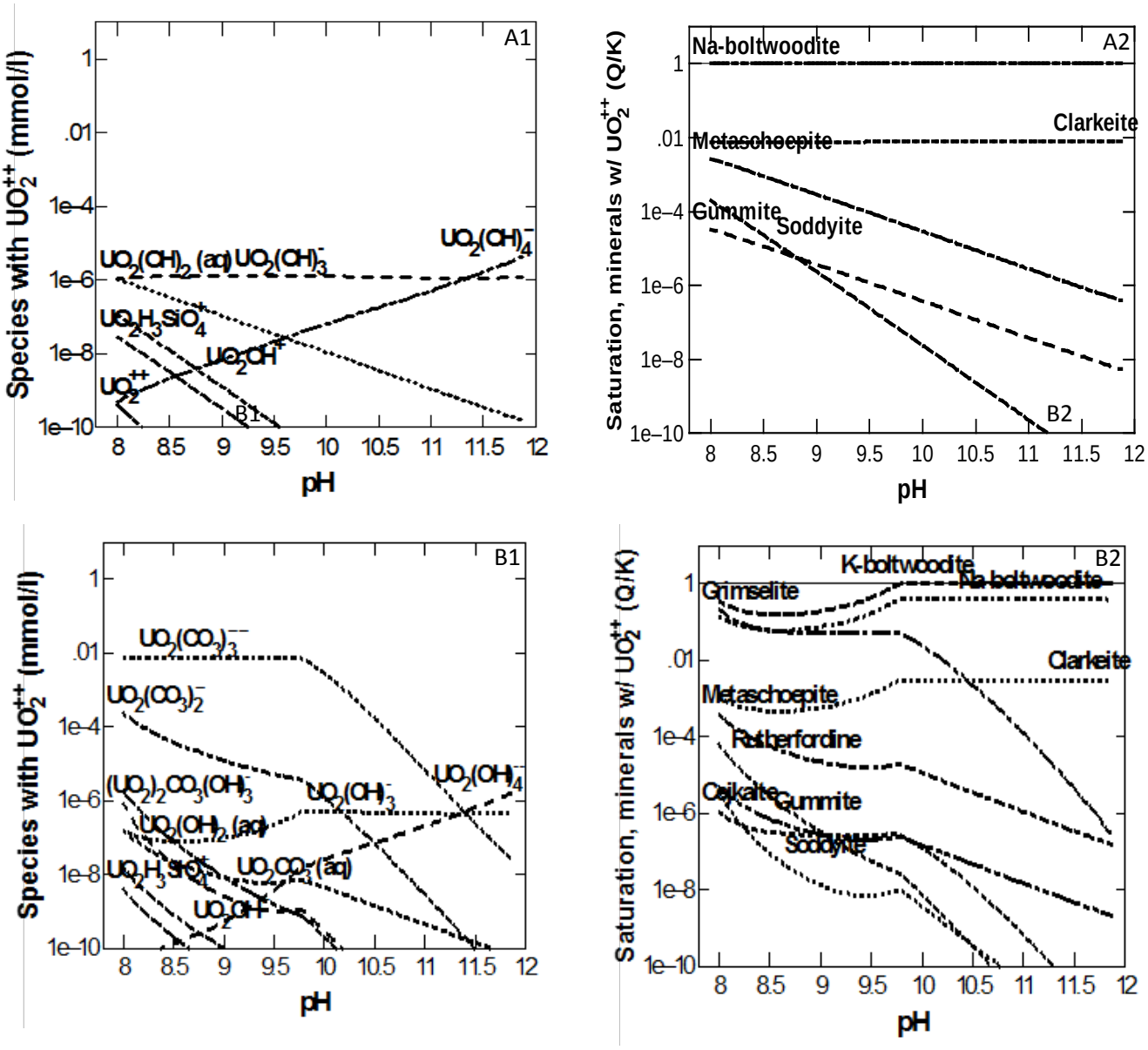

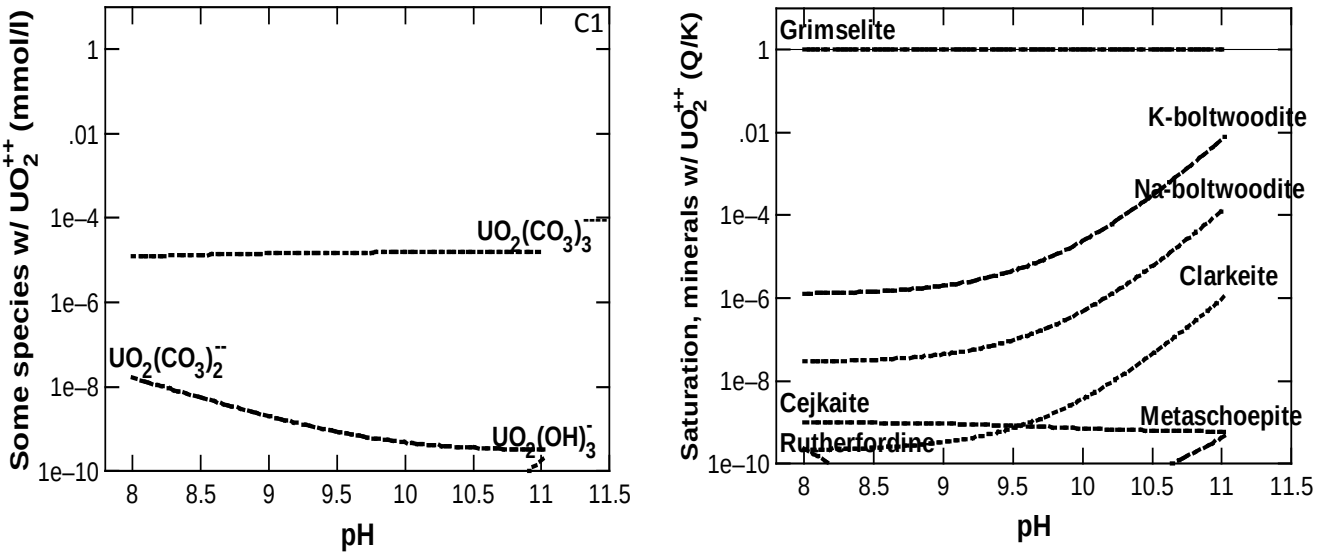


Figure 1. Diagrams of uranium aqueous species and saturation indices of some of uranium-bearing mineral phases plotted as a function of pH for 5% of $NH_3$ (3.1mol/L $NH_3$(aq)). Sample composition includes 50mM of Si and varied $HCO_3^-$ concentrations. The first row shows diagrams for $HCO_3^-$free samples (A1, A2), the 2nd and 3rd row show the diagrams for 2.9mM (B1, B2) and 50mM of $HCO_3^-$ (C1, C2).

Modeling also predicted the formation of relevant uranyl mineral phases. For the Ca –free samples, modeling predicted the formation of uranyl solid phases such as uranyl silicates, (NaK)boltwoodite [$(Na,K)(UO_2)(HSiO_4)\cdot 0.5H_2O$], in addition to uranyl carbonates, grimselite [$K_3Na(UO_2)(CO_3)_3\cdot(H_2O)$], cejkaite [$Na_4(UO_2)(CO_3)_3$ and rutherfordine [$UO_2(CO_3)$] as well as uranyl oxide hydrates, metaschoepite [$(UO_2)_8O_2(OH)_{12}(H_2O)_{12}$] and clarkeite [$Na(UO_2)(2H_2O)$. Na-boltwoodite was present in all of the conditions tested, while rutherfordine and grimselite were seen only in the presence of low (2.9 mM) and high (50 mM) bicarbonate concentrations, respectively. For the formation of uranyl hydroxide minerals, metaschoepite was favored under bicarbonate-free and 2.9 mM bicarbonate concentrations; however, its saturation indices decreased as the concentration of bicarbonate ions increased. SI of Na-boltwoodite were found to be the highest for bicarbonate- free and 2.9 mM concentrations.

## Speciation modeling for Ca-amended synthetic solutions

GWB simulations were conducted for synthetic mixtures composed of 50 mM Si and 10 mM of Ca. Three bicarbonate concentrations were chosen for the experiments: 0 mM, a “low” bicarbonate concentration of 2.9mM and a “high” bicarbonate concentration of 50 mM. The Al concentration of 5 mM was constant for all simulations.

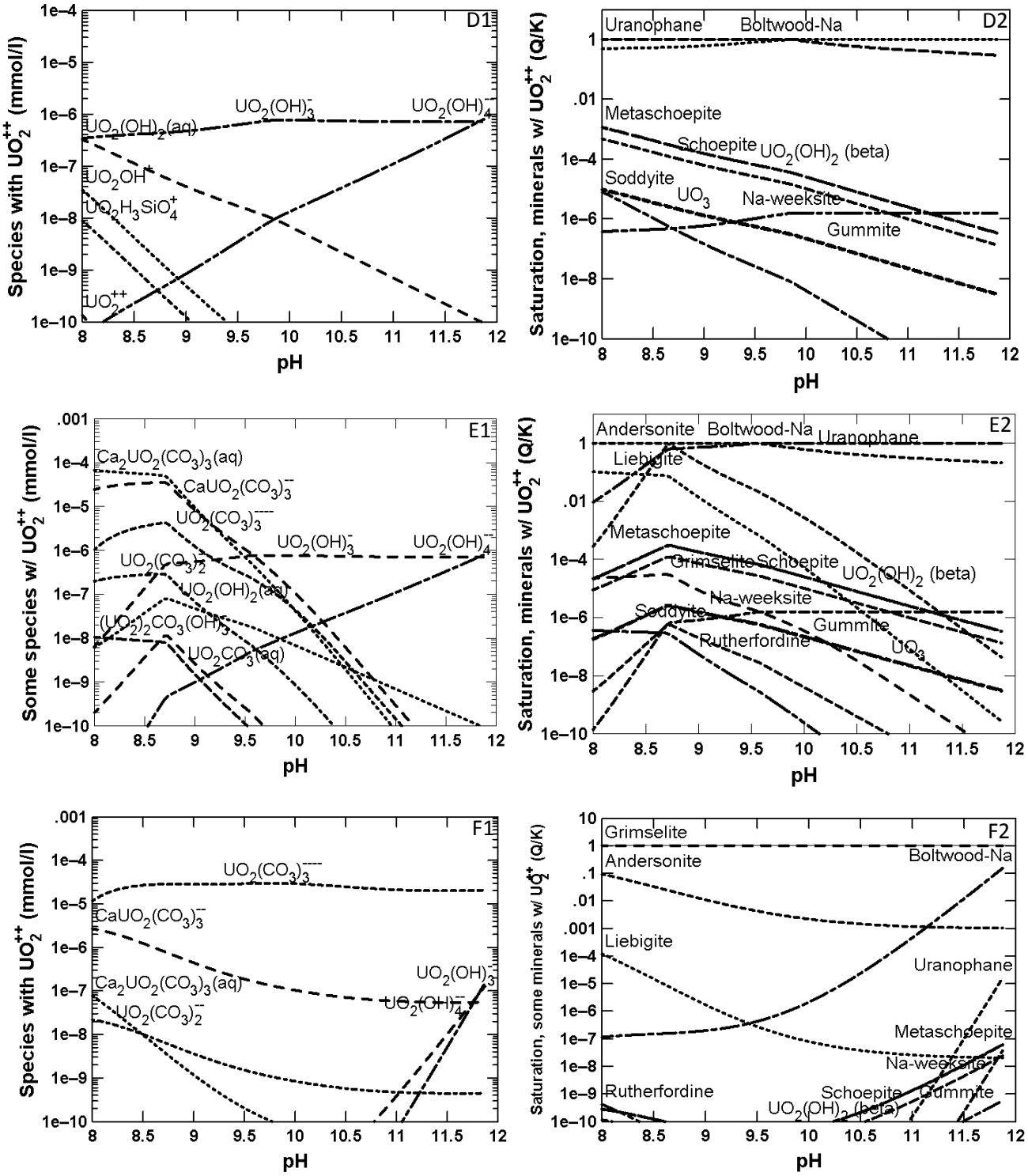


Figure 2. Diagrams of uranium aqueous species and saturation indices of some of uranium-bearing mineral phases plotted as a function of pH for 5% of $NH_3$ (3.1 mol/L $NH_3$(aq)). Sample composition includes 50mM of Si, 10mM of Ca and varied $HCO_3^-$ concentrations. The first row shows diagrams for $HCO_3$—free samples (D1, D2), the 2nd and 3rd row show the diagrams for 2.9mM (E1, E2) and 50mM of $HCO_3^-$ (F1, F2).

Modeling simulations predicted the highest saturation indices for uranyl silicate solid phases, Na-boltwoodite and uranophane, at bicarbonate-free conditions. Uranyl carbonate solid phases, andersonite and liebigite, were found at the low bicarbonate concentration and grimselite was seen at the high bicarbonate concentration of 50 mM (Figure 2-C1, C2). The uranyl oxide hydrates, metaschoepite, was predicted to be under saturated (SI<1) at bicarbonate-free and low bicarbonate concentrations of 2.9 mM. Aqueous speciation at low bicarbonate concentrations were dominated by calcium uranyl carbonates aqueous species until pH 9.5; at higher pH, the dominant species were uranyl hydroxides (Figure 2- B1, B2).

The studies also attempted to determine the morphological and mineralogical characteristics of the uranium solid phases produced during ammonia treatment. SEM and EDS analysis were used for the observation of uranium phases (Figure 3) to select samples for XRD analysis. The grounded samples prepared with high bicarbonate concentrations (50 mM) showed the uranium-bearing dense regions of amorphous collection. EDS analysis of these areas resulted in uranium weight percentages of 12.38% (Figure 3).

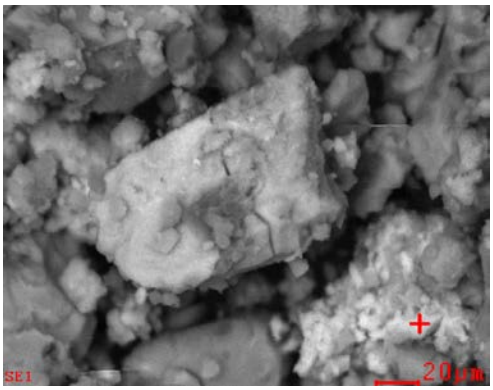

| Element | Wt% | At% |
|---|---|---|
| CK | 07.66 | 13.41 |
| NK | 04.98 | 07.47 |
| OK | 38.90 | 51.12 |
| NaK | 06.82 | 06.24 |
| AlK | 02.30 | 01.79 |
| SiK | 20.25 | 15.16 |
| ClK | 02.49 | 01.47 |
| KK | 01.61 | 00.87 |
| CaK | 02.61 | 01.37 |
| UL | 12.38 | 01.09 |
| Matrix | Correction | ZAF |

Figure 3. SEM image showing the crystalline uranium phases and the spot chemical composition using EDS. Sample was composed using 50mM of Si, 5mMAl, 10mM of Ca and 50mM $HCO_3$.

The low bicarbonate version exhibited similar amorphous uranium-dense areas with comparable U weight percentages of 11.42% (Figure 4). These areas coincided with a higher Si weight percentage (21%).

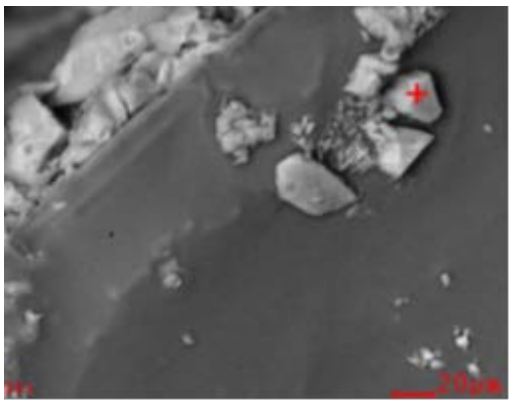

| Element | Wt% | At% |
|---|---|---|
| CK | 14.60 | 31.53 |
| OK | 10.80 | 17.50 |
| NaK | 02.51 | 02.83 |
| AlK | 02.14 | 02.05 |
| SiK | 21.06 | 19.45 |
| ClK | 12.13 | 08.87 |
| UM | 11.42 | 01.24 |
| KK | 06.10 | 04.05 |
| CaK | 19.26 | 12.46 |
| Matrix | Correction | ZAF |

Figure 4. SEM image of the grounded precipitate sample and the spot composition using EDS. Sample was composed using 50mM of Si, 5mM Al, 10mM of Ca and 3mM $HCO_3$.

The presence of boltwoodite and uranophane were predicted by the speciation modeling and SEM/EDS identified areas of concentrated uranium and Si. However, uranyl silicates were not detected with any certainty by powder XRD, perhaps due to the amorphous nature of these solid phases (data not shown).

## CONCLUSIONS

Diagrams with aqueous uranium species plotted as a function of pH showed that in bicarbonate–free synthetic solutions, $UO_2(OH)_3^-$ and $UO_2(OH)_4^{2-}$ were the predominant aqueous uranium species. In the presence of bicarbonate, aqueous uranium carbonates species, $UO_2(CO_3)_3^{4-}$ and $UO_2(CO_3)_2^{2-}$, dominated uranium speciation. In calcium-amended solutions, aqueous speciation at low bicarbonate concentrations were dominated by calcium uranyl carbonates species until pH 9.5; at higher pH, the major species were uranyl hydroxides. In the absence of calcium, Na- and K- boltwoodite were the prevailing solid phases at low and bicarbonate-free conditions. In the presence of Ca ions in the solutions, speciation modeling predicted the formation of uranophane solid phases. At higher bicarbonate concentrations, grimselite was found to be a predominant solid phase for all tested scenarios. Speciation modeling of uranium –containing pore water was conducted for various $Ca^{2+}$ and bicarbonate concentrations as a function of pH. This can predict the formation of potential U(VI) aqueous species and solid phases created after the application of ammonia gas under the Hanford Site's vadose zone conditions.

## ACKNOWLEDGEMENTS

Funding for this research was provided by U.S. DOE cooperative agreement DE-EM0000598.

## REFERENCES

1. Szecsody, J. E., Truex, M. J., Qafoku, N. P., Wellman, D. M., Resch, T., & Zhong, L. R. (2013). Influence of acidic and alkaline waste solution properties on uranium migration in subsurface sediments. *Journal of Contaminant Hydrology, 151*, 151-175.
2. Zachara, J. M., Brown, C., Christensen, J., Davis, J. A., Dresel, E., Liu, C., Um, W. (2007). A site-wide perspective on uranium geochemistry at the Hanford site. (No. PNNL-17031). Richland, Washington: Pacific Northwest National Laboratory.
3. Zachara, J. M., Davis, J. A., McKinley, J. P., Wellman, D. M., Liu, C., Qafoku, N. P., & Yabusaki, S. (2005). *Uranium geochemistry in vadose zone and aquifer Sediments from the 300 area uranium plume.* (No. PNNL-15121). Richland, Washington: Pacific Northwest National Laboratory (PNNL).
4. Langmuir, D. (Ed.).*Aqueous environmental geochemistry* Prentice Hall, Upper Saddle River, NJ.
5. Guillaumont, R., Fanghänel, T., Fuger, J., Grenthe, I., Neck, V., Palmer, D., & Rand, M. (2003). Update on the chemical thermodynamics of U, Np, Pu, Am and Tc.

6. Szecsody, J. E., Truex, M. J., Zhong, L., Johnson, N. P., Qafoku, N. P., Williams, M. D., Faurie, D. K. (2012). Geochemical and geophysical changes during ammonia gas treatment of vadose zone sediments for uranium remediation. *Vadose Zone Journal,* , 1-13.
7. Zhong, L., Szecsody, J. E., Truex, M. J., Williams, M. D., & Liu, Y. (2015). Ammonia gas transport and reactions in unsaturated sediments: Implications for use as an amendment to immobilize inorganic contaminants. *Journal of Hazardous Materials, 289*, 118-119.
8. Bickmore, B. R., Nagy, K. L., Young, J. S., & Drexler, J. W. (2001). Nitrate-cancrinite precipitation on quartz sand in simulated hanford tank solutions. *Environmental Science & Technology, 35*, 4481-4486.
9. Qafoku, N. P., Ainsworth, C. C., Szecsody, J. E., & Qafoku, O. S. (2004). Transport-controlled kinetics of dissolution and precipitation in the sediments under alkaline and saline conditions. *Geochimica Et Cosmochimica Acta, 68*, 2981-2995.
10. Qafoku, N. P., & Icenhower, J. P. (2008). Interactions of aqueous U (VI) with soil minerals in slightly alkaline natural systems. *Reviews in Environmental Science and Bio/Technology, 7*, 355-380.
11. Serne, R., Last, G. V., Horton, D., Gee, G. W., Schaef, D. E., Lanigan, D. C., Orr, R. D. (2008). Characterization of vadose zone sediment: Borehole 299-E33-45 near BX-102 in the B-BX-BY waste management area. (No. PNNL-14083). Richland, WA.
12. Katsenovich, Y. P., Cardona, C., Lapierre, R., Szecsody, J., & Lagos, L. (2016). The effect of si and al concentrations on the removal of U (VI) in the alkaline conditions created by NH3 gas. Applied Geochemistry, 73, 109-117.
13. Zhong, L., Szecsody, J. E., Truex, M. J., Williams, M. D., & Liu, Y. (2015). Ammonia gas transport and reactions in unsaturated sediments: Implications for use as an amendment to immobilize inorganic contaminants. Journal of Hazardous Materials, 289, 118-119.
14. Szecsody, J. E., Truex, M. J., Zhong, L., Qafoku, N., Williams, M. D., McKinley, J. P., Phillips, J. L. (2010). Remediation of uranium in the Hanford vadose zone using ammonia gas: FY 2010 laboratory-scale experiments. medium. (No. PNNL-20004). Richland, WA.: Pacific Northwest National Laboratory.
15. Qafoku, N. P., Ainsworth, C. C., Szecsody, J. E., & Qafoku, O. S. (2003). Aluminum effect on dissolution and precipitation under hyperalkaline conditions. Journal of Environmental Quality, 32, 2354-2363.
16. Liu, C., Zachara, J. M., Qafoku, O., McKinley, J. P., Heald, S. M., & Wang, Z. (2004). Dissolution of uranyl microprecipitates in subsurface sediments at hanford site, USA. Geochimica Et Cosmochimica Acta, 68, 4519-4537.
17. Bethke, C. M. (Ed.). (2007). *Geochemical and biogeochemical reaction modeling* (2nd ed.) Cambridge University Press.
18. Hummel, W., Berner, U., Curti, E., Pearson, F., & Thoenen, T. (2002). Nagra/PSI chemical thermodynamic data base. *National Cooperative for the Disposal of Radioactive Waste in Switzerland (Nagra), 02-16*
19. Richter, A., Bok, F., & Brendler, V. (2015). *Data compilation and evaluation for U(IV) and U(VI) for the thermodynamic reference database THEREDA.* (No. HZDR-065). Dresden: Helmholtz Zentrum Dresden - Rossendorf.

20. Grenthe, I., Fuger, J., Konings, R. J., Lemire, A. B., Muller, C., Nguyen-Trung, C., & Wanner, H. (1992). Chemical thermodynamics of uranium.1.
21. Kalmykov, S. N., & Choppin, G. R. (2000). Mixed $Ca^{2+}/UO_2^{2+}/CO_3^{2-}$complex formation at different ionic strengths. *Radiochimica Acta International Journal for Chemical Aspects of Nuclear Science and Technology, 88*, 603-606.
22. Bernhard, G., Geipel, G., Reich, T., Brendler, V., Amayri, S., & Nitsche, H. (2001). Uranyl (VI) carbonate complex formation: Validation of the $Ca_2UO_2(CO_3)_3$(aq) species. *Radiochimica Acta International Journal for Chemical Aspects of Nuclear Science and Technology, 89*, 511.
23. Dong, W., & Brooks, S. C. (2006). Determination of the formation constants of ternary complexes of uranyl and carbonate with alkaline earth metals ($Mg^{2+}$, $Ca^{2+}$, $Sr^{2+}$, and $Ba^{2+}$) using anion exchange method. *Environmental Science & Technology, 40*, 4689-4695.
24. Gorman-Lewis, D., Burns, P. C., & Fein, J. B. (2008). Review of uranyl mineral solubility measurements. *Journal of Chemical Thermodynamics, 40*(3), 335-352. doi:http://dx.doi.org/10.1016/j.jct.2007.12.004
25. Thoenen, T., Hummel, W., Berner, U., & Curti, E. (2014). *PSI/Nagra chemical thermodynamic database.* ( No. 12/07). Switzerland: Paul Scherrer Institut (PSI).
26. Felmy, A. R., Cho, H., Rustad, J. R., & Mason, M. J. (2001). An aqueous thermodynamic model for polymerized silica species to high ionic strength. *Journal of Solution Chemistry, 30*, 509-525.
27. Shvareva, T. Y., Mazeina, L., Gorman-Lewis, D., Burns, P. C., Szymanowski, J. E., Fein, J. B., & Navrotsky, A. (2011). Thermodynamic characterization of boltwoodite and uranophane: Enthalpy of formation and aqueous solubility. Geochimica Et Cosmochimica Acta, 75(18), 5269-5282. doi:http://dx.doi.org/10.1016/j.gca.2011.06.041